

## **APPLICATIONS OF GROUND PENETRATING RADAR AND MICROWAVE TOMOGRAPHY IN WATER MONITORING AND MANAGEMENT**

*F. Soldovieri<sup>1</sup>, L. Crocco<sup>1</sup>, A. Brancaccio<sup>2</sup>, R. Solimene<sup>2</sup> and R. Persico<sup>3</sup>*

<sup>1</sup>Institute for Electromagnetic Sensing of the Environment, soldovieri.f@irea.cnr.it

<sup>2</sup> Second University of Naples, adriana.brancaccio@unina2.it

<sup>3</sup>Institute for Archaeological and Monumental Heritage, r.persico@ibam.cnr.it

### **ABSTRACT**

*Ground Penetrating Radar (GPR) is one of the most widely exploited diagnostics tools in the fields of the water monitoring and management as well as in the recent application fields of the agricultural geophysics.*

*In this work, we present the most recent results concerning with a state of art data processing for GPR based on accurate models of the inverse scattering at the basis of the sensing phenomenon. In particular, we will present the successful cases of the use of a microwave tomographic approach in the cases of drainage pipe location, water leaks from pipes monitoring and determination of the water content in the soil.*

**Keywords:***Ground Penetrating Radar, water content, pipes detection and characterization, inverse scattering, microwave tomography.*

### **1. INTRODUCTION**

Ground Penetrating Radar (GPR) (Daniels [1]) is a well assessed diagnostic instrumentation that finds application in a very large range of sectors when the objective is of achieving information about the presence, the position and the morphological properties of targets embedded in opaque media. Therefore, it is of interest in many sectors ranging from civil engineering diagnostics (Hugenschmidt and Kalogeropoulos [2]);, to archaeological prospecting (Conyers and Goodman,[3]), to cultural heritages management, to geophysics, only to quote a few examples.

GPR is also one of the most used tools in the field of the water monitoring and management especially in the fields of the drainage pipes detection and characterization (Allred et al. [4]), water leaks in pipe detection (Crocco et al. [5]), determination of the time-behavior of water content in the soil (Lambot et al. [6], Lambot et al. [7]).

The widely use of GPR is due to the some advantage offered by the GPR instrumentation that can be stated as the low cost and easiness of employ. In fact no particular expertise is required to collect the data. Secondly, the instrumentation is easily portable (unless very low frequencies are exploited thus increasing the physical size of the antennas) and allows to survey regions also of thousands of square metres in reasonable time. Finally, the flexibility of the GPR system is ensured by the adoption of antennas (mostly portable) working at different frequencies and that can be straightforwardly changed on site.

It is worth noting that the necessities of probing lossy medium and of achieving resolution of the order of centimetres poses a very challenging task for the antennas deployed in the survey. On the other hand, as mentioned above, the portability of the system has to be ensured so that no complicated and large antenna systems can be employed. In particular, the trade-off between the necessity to have a large investigation range (that pushes to keep low the operating frequency) and the aim of achieving good spatial resolution makes the overall working frequency band exploited by GPR systems ranging from some tens of MHz to some GHz.

Despite of the said above advantages, the main limitation affecting the use of GPR resides in the fact that the raw data (given usually under the form of a radargram) is difficult to be interpreted in order to achieve clear and accurate information about the investigated scene in terms of presence, location and geometry of the buried objects (Daniels [1]). Such a direct “interpretation” is usually based on the available a priori information on the investigated scene and on the expertise of the final end-user. In the more complicated cases, such an interpretation reveals very challenging and this affects the overall reliability and accuracy of the GPR measurement survey. According to the above said drawbacks, the necessity arises of developing and analyzing automatic processing approaches able to give clearer, clever and more stable and interpretable reconstructed images compared to the starting raw-data. In the last years, a class of solution approaches based on RF/microwave tomography have gained increasing interest. Microwave tomography technique has become an increasingly popular interpretational tool for GPR applications. In fact, the possibility of recasting the data processing as an inverse scattering problem (Colton and Kress [8]) leads to an improvement of the interpretation of simpler radargrams. In addition, the adoption of more accurate models of the electromagnetic scattering phenomenon can help us to understand crucial aspects of a specific problem at a much deeper interpretational level. In addition, the theoretical investigation of the inverse scattering problem enables us to evaluate the reconstruction performances in term of example of available resolution limits achievable in a reconstructed image, and to give guidelines about spatial and frequency sampling to be adopted in the survey criteria (Leone and Soldovieri [9], Persico et al. [10])

In this contribution, we will present the exploitation of the microwave tomographic approach for GPR data processing in the context of the water monitoring and management and agricultural geophysics. Therefore, the paper is organized as follows. Section 2 is devoted at presenting the formulation of the inverse scattering approach in the simplified configuration (any way suitable for many applications) of 2D geometry. In Section 3 we show some example results achieved by the microwave tomographic approach in some application fields such as: pipe detection and characterization and water content determination t. Finally Conclusions follow.

## 2. THE MICROWAVE TOMOGRAPHIC APPROACH

This Section is devoted at presenting a widely used inverse scattering approach based on a simplified model of the electromagnetic scattering. In particular, here we deal with the microwave tomographic approach based on the Born Approximation (BA) has been already presented in many papers (Leone and Soldovieri [9]; Persico et al. [10]), here the approach is briefly recalled.

The geometry of the problem is presented in the Figure 1 and is concerned with a half-space homogeneous scenario and two-dimensional geometry. The adopted measurement configuration is usually the multi-monostatic/multi-frequency one: this means that the GPR system moves at the interface air/soil when the location of the transmitting and receiving antennas coincide.

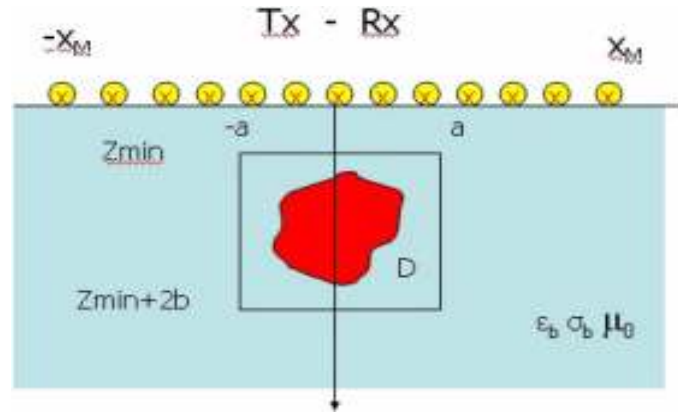


Fig. 1 Geometry of the problem

The scattered field is given as the ‘difference’ between the total field and the unperturbed field  $E_{inc}$ . The total field is the field reflected by the soil when buried objects are present, whereas the unperturbed field is the field reflected by the soil when the objects are absent and, therefore, it accounts for reflection/transmission at the air/soil interface. The targets are assumed to be invariant along the  $y$ -axis and their cross-section is assumed to be included in a rectangular investigation domain  $D$ . The unknowns of the problem are the *relative dielectric permittivity and the conductivity* spatial distributions inside  $D$ . Under BA, the relationship between the unknown contrast function and the scattered field data is provided by the integral equation (Leone and Soldovieri [9]):

$$E_s(x_s, \omega) = k_s^2 \int_D G_e(x_s, \omega, \vec{r}') E_{inc}(x_s, \omega, \vec{r}') \chi(\vec{r}') d\vec{r}' \quad (1)$$

The ‘unknown’ is the contrast function  $\chi$  that accounts for the relative difference between the equivalent dielectric permittivity of the objects  $\epsilon_{object}(\vec{r}')$  and the one of the embedding medium  $\epsilon_b$ :

$$\chi(\vec{r}') = \frac{\epsilon_{object}(\vec{r}')}{\epsilon_b} - 1 \quad (2)$$

$G_e(\cdot)$  is Green’s function,  $E_{inc}$  is the incident field and  $k_s$  is the wave-number of the investigated medium (Leone and Soldovieri [9]).

The linear integral relation in (1) is inverted by means of the Singular Value Decomposition (SVD) tool that allows to achieve a stable solution (Bertero [11]). Finally, the result of the reconstruction is represented as the spatial map of the modulus of the SVD-recovered contrast function within the region under investigation.

Figure 2 summarizes and sketches the overall processing chain to obtain the microwave tomographic reconstruction starting from the time-domain raw data.

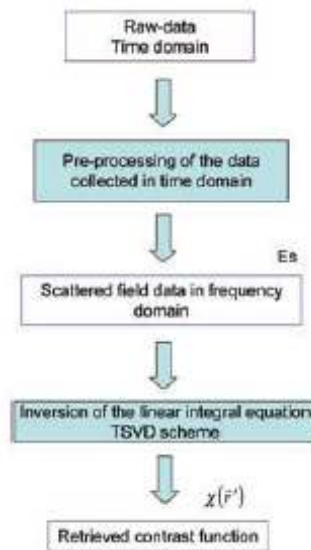


Fig. 2 The processing chain from the time-domain raw data to the contrast function

Finally, it is worth noting that if we have presented a MT approach based on Born Approximation, similar approaches also have been developed in the case of metallic objects (strongly scattering objects) based on Kirchhof Approximation (Pierri et al. [12]).

### 3. EXAMPLES OF THE APPLICATION OF THE MICROWAVE TOMOGRAPHIC APPROACH IN WATER MONITORING

This section is devoted at presenting some examples of the results achieved by the Microwave Tomographic (MT) approach in the fields of the pipe detection and characterization and water content. The Section has been divided in Subsections dealing separately the presented cases.

#### 3.1 Pipe detection and characterization

MT approach has been applied with success in realistic cases regarding the pipe detection and characterization in terms of geometrical parameters (location and shape). Figure 3 depicts the 3D reconstruction of a pipe of 0.25-m diameter buried at a depth of approximately 50 cm. The measurement data have been collected at the Annunziata Cloister, Second University of Naples, and are part of a survey that has been performed with the aim of detecting and localizing buried utilities. The measurements were collected by means of the RIS-K2 model of IDS equipped with a 200-MHz antenna. The 3D reconstruction was achieved by joining the 2D reconstruction of seven scans (vertical profiles) equally spaced from each other at a distance of about 50 cm for a total length of 3 m. (Soldovieri et al. [13], Solimene et al. [14])

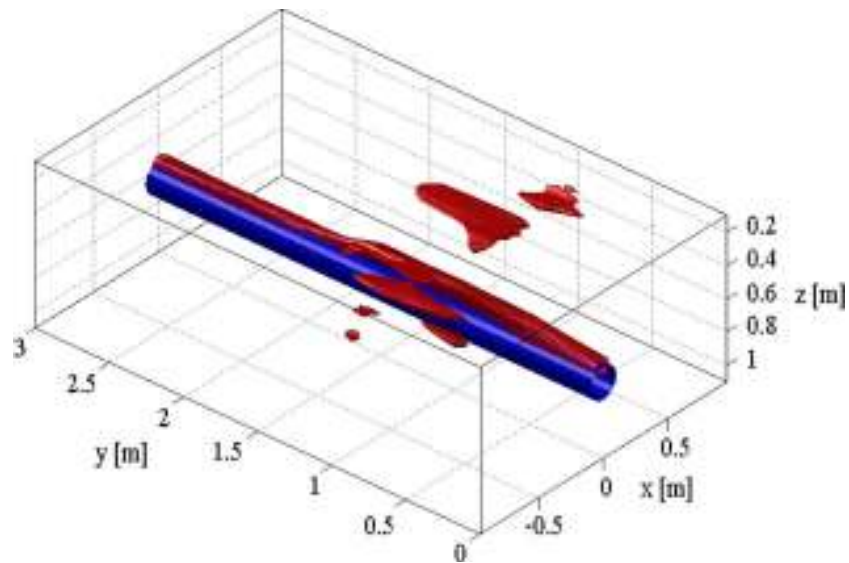


Fig. 3 (Red) Three-dimensional image of the (blue) pipe as a result of the superposition of all the 2-D reconstructions (scans from S1 to S7).

Let us turn now to present a result stating the possibility of the MT to infer information (in terms of dielectric permittivity) about the liquid filling the pipe once one knows the geometry of the pipe (Pettinelli et al. [15]).

Fig. 4 shows the tomographic reconstruction of the plastic pipe filled with water. Two clear localized high-amplitude zones are visible on the image (pointed out by the back arrows). The shallower zone (upper arrow) gives a good localization of the top of the pipe, which is consistent with the depth given by raw data. Moreover, the good focusing effect that is observable on the image allows for a dimension estimation of the cross section of the pipe. The zone at a depth of about 1.95 m (lower arrow) corresponds to the bottom part of the plastic pipe. The distance between the two maxima of the modulus of the retrieved contrast function can be estimated as equal to 0.62 m whereas the actual diameter of the pipe is 0.16 m. This difference between the true and retrieved distances is due to the change in the dielectric properties of the medium inside the pipe with respect to the one of the surrounding medium.

In fact, the Born inversion model assumed for the soil has a relative dielectric permittivity that is equal to 4.7, so that the wave velocity is approximately 14 cm/ns. On the other hand, the electromagnetic wave propagates across the water filling the pipe with a velocity of 3.4 cm/ns (assuming a value of 79 for the relative dielectric permittivity of water). Therefore, theoretically, the distance between the top and the bottom of the pipe can be calculated as follows:  $\sqrt{79/4.7} * 0,16 = 0,65$  m which gives a value that is very close to 0.62 m.

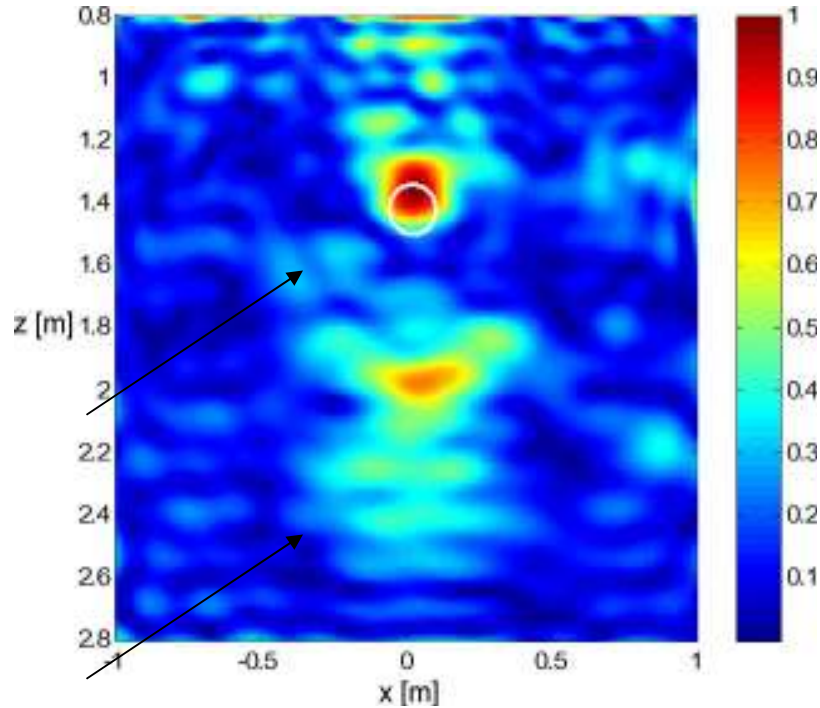


Fig.4 Reconstruction of the normalized amplitude of the contrast function for the water-filled pipe.

### 3.2. Detection and characterization of water leakage in pipe

Distorted wave models (Chew [16]) are often adopted in inverse scattering with the aim of reducing the complexity of the problem and improving the reliability and stability of the solution approaches, thanks to the exploitation of a priori information on the scenario under investigation.

In particular, for the case at hand, one can take advantage of the available knowledge on the pipe's position and size to overcome the fact the field backscattered by the pipeline in most cases overwhelms the one scattered by the leakage, unless this latter is large, thus precluding timely detection. Hence, rather than considering the "conventional" homogeneous half-space reference scenario adopted in standard microwave tomographic techniques for GPR applications and presented in the section below, one can formulate the inverse scattering problem within a background scenario wherein the pipe features are assumed to be known and included in the background scenario, while the leak represents the only "anomaly" (Crocco et al. [5]).

Here, we present the validation of the distorted approach with synthetic data. The simulations consist of a shielded dipole antenna, having a central frequency of 900 MHz, which radiates over a 0.12m diameter, circular, water-filled metal pipe buried to a depth of 0.5m in a dry, low- to-medium loss, uniform sandy soil of relative permittivity about equal to 3 and a static conductivity of  $\sigma = 10$  mS/m. The temporally and spatially varying water leakage has been modelled as an incipient, low-flow, low-pressure, gravity-fed leak that emanates from the base of the pipe and soaks the surrounding sands in an expanding saturation front that moves both laterally and vertically downwards across the modelled volume. The saturated soils have frequency-dependent dielectric properties with a relative dielectric permittivity of approximately 22 at 900 MHz. The synthetic data have been corrupted with an additive Gaussian noise with a signal-to-noise ratio of 20 dB.

The results of the inversion algorithm in the three cases are reported in Fig. 5. As can be seen, the approach is able to detect/localize the leak and estimate its extent for both the large and medium leakage examples, (Fig. 5(a) and Fig. 5(b)). As shown in Fig. 5(c), even in the small leak case, where the leak is almost completely masked by the pipe, the presence of an anomaly is clearly detected, thus illustrating the early-time warning capability of the method and its ability to track the evolving leak from its inception.

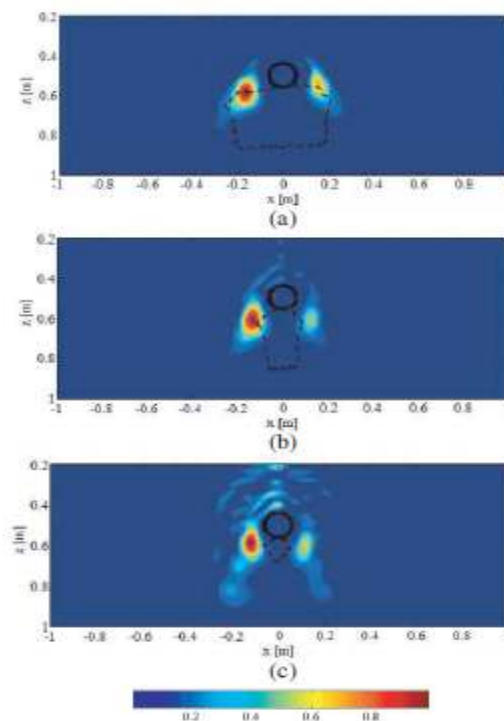


Fig. 5 Normalized modulus of the reconstructed contrast achieved through the distorted wave tomographic approach in the three cases of a (a) large; (b) medium, and (c) small leak.

### 3.3. Determination of water content by a auto-focusing approach

In this subsection, we present an approach dealing with the problem of the determination the electromagnetic properties of the soil (dielectric permittivity and electrical conductivity) starting from the GPR measurements of the field backscattered by a buried cooperative target that has a cross-section small in terms of the probing wavelength (Soldovieri et al [17]). To do this, we reverse the point of view adopted in the subsections below and try to determine the dielectric permittivity of the soil as the value that, when introduced in the integral Eq. (1), drives to the “reconstruction” closest to the known buried target, embedded in the soil on the purpose. Consequently, the problem of how quantifying the quality of the reconstruction arises, i.e. we have to identify a figure of merit that makes us able to characterize the “best” reconstruction.

According to the consideration above, here we adopted a different point of view where the goodness of the reconstruction is evaluated in terms of others features related to the actual distribution of the contrast function. This point of view is exploited in radar and optics literature where the goodness of the reconstruction is evaluated in terms of the sharpness (Ahmad et al. [18]), the compactness, the entropy (Martorella [19]), the spectral features, only to quote few examples.

In the case of a lossless or with low ohmic losses soil, we have seen that a criterion to evaluate the most focused image (at variance of the soil dielectric permittivity assumed in the Born model) is based on a sharpness measure  $\text{Sharp}(\epsilon_b, \sigma_b)$  accounting for the maximum of the modulus of the reconstructed contrast function (Soldovieri et al. [17]) and where the soil dielectric permittivity and electrical conductivity are denoted by  $\epsilon_b$  and  $\sigma_b$  respectively. Therefore, in the lossless cases, a good criterion to retrieve the permittivity is to retain the model permittivity that allows to achieve the maximum value (vs. the model permittivity) of the maximum modulus of the contrast function (vs. the point in the investigation domain  $D$ ). (Soldovieri et al. [20]) Now, the estimated value of the dielectric permittivity and conductivity are chosen as the ones that maximize the  $\text{Sharp}(\epsilon_b, \sigma_b)$  function. This approach has been tested numerically even in lossy cases, but only in situations where the conductivity of the soil was accurately known, and in this case the approach works in a satisfactory way.

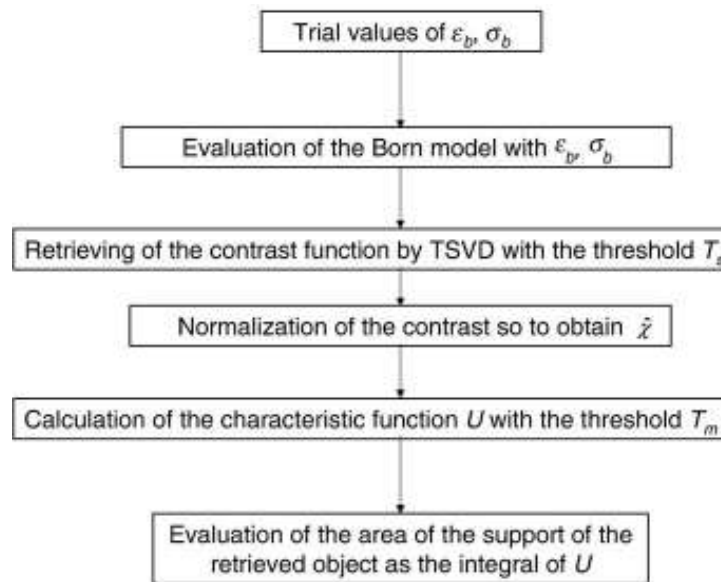


Fig. 6 Flow chart depicting the determination of the area of the support as the integral of the characteristic function

However, in the realistic cases the conductivity of the soil is known with some degree of uncertainty, and this can make unreliable the determination of the dielectric permittivity based on the previous criterion. Thus, the need to establish a different criterion which mitigates the effects of the inaccurate knowledge of the soil conductivity. According to the above analysis, in the case of uncertainty in the knowledge of the soil conductivity, the exploited figure of merit (maximum of the modulus of the contrast function) to quantify the degree of focalisation, based on the level of the retrieved contrast, is not adequate. Therefore here, we propose a new figure of merit that we will label as “the criterion of the minimum support”, that is based on the determination of the area of the support of the retrieved contrast function. In order to do this, we assume that the buried pipe is most focused when the area of the reconstructed spot is “minimum”. The flow chart of the determination of the support is depicted in figure 6.

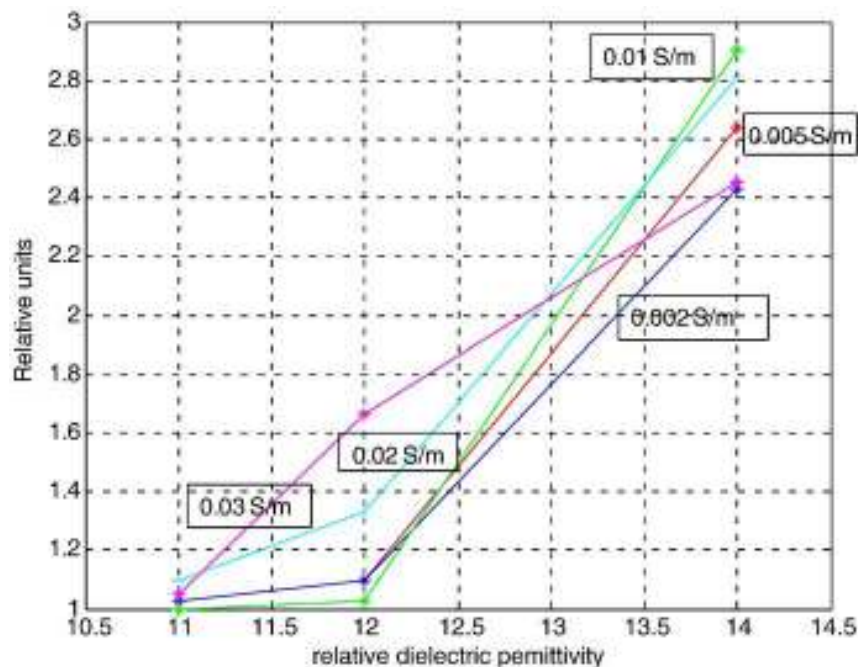


Fig. 7 The estimated area of the retrieved support of the contrast function for each pair of the trials values of the dielectric and conductivity.

The effectiveness of the “minimum support” criterion is shown here with synthetic test cases. In particular, we have considered the case of a soil with true relative dielectric permittivity equal to 12 and conductivity equal to 0.01 S/m. The buried object is a metallic pipe with circular cross-section with radius of 0.05 m and whose centre is at the depth of 0.6 m. The scattered field is measured over an observation domain with extent 1.6 m in 41 equally spaced points; the work frequency ranges from 100 MHz to 800 MHz with a step of 20 MHz. In particular, we consider the case of three trial values of the soil relative dielectric permittivity (11, 12, 14) and five different trial values of the soil conductivity (0.002, 0.005, 0.01, 0.02, 0.03 S/m).

Figure 7 allows us to state the reliability of the criterion of the minimum support in the case of an accurate choice of the conductivity (see the green curve corresponding to 0.01 S/m). Also Fig. 7 shows that the behaviour of the lines between  $\epsilon_b=11$  and  $\epsilon_b=12$  is less sensible to the model conductivity, except in the case of  $\sigma_b=0.03$ , which is a strongly over-estimated conductivity.

## 5. CONCLUSIONS

We have presented how the application of the microwave tomographic approach allows to obtain good focused images of the buried targets (pipes), thus permitting an accurate detection and geometry estimation of the targets and the liquid filling them.

Furthermore, we have presented a soil electromagnetic properties estimation based on the auto-focussing strategy and microwave tomography approach.

## REFERENCES

- [1] Daniels, D. J., 2004, *Ground Penetrating Radar*. IEE Radar, Sonar and Navigation Series, London.
- [2] Hugenschmidt, J. and Kalogeropoulos, A., 2009, The inspection of retaining walls using GPR, *Journal of Applied Geophysics*, 67, pp. 335-344.
- [3] Conyers, L. B. and Goodman, D., 1997, *Ground Penetrating Radar: An Introduction for Archaeologists*. Alta Mira Press, Walnut Creek, London and New Delhi.
- [4] Allred, B.J., Daniels, J.J., Ehsani, M.R., 2008, *Handbook of Agricultural Geophysics*, CRC Press, ISBN:9780849337284.
- [5] Crocco, L., Soldovieri, F., Millington, T., and Cassidy, L., 2010, Bistatic tomographic GPR imaging for incipient pipeline leakage evaluation, *Progress In Electromagnetics Research*, PIER 101, 307-321
- [6] Lambot, S.; Slob, E. C., Chavarro, D., Lubczynski, M., and Vereecken, H., 2008, Measuring soil surface water content in irrigated areas of southern Tunisia using full-wave inversion of proximal GPR data. *Near Surface Geophysics*, 16, 403-410.
- [7] Lambot, S., Slob, E.C., van den Bosch, I., Stockbroeckx, B., Vanclooster, M., 2004, Modeling of ground-penetrating radar for accurate characterization of subsurface electric properties. *IEEE Transaction on Geoscience and Remote Sensing*, 42, 2555–2568.
- [8] Colton, D. and Kress, R., 1992, *Inverse Acoustic and Electromagnetic Scattering Theory*. Springer-Verlag, Berlin.

- [9] Leone, G., Soldovieri, F., 2003. Analysis of the distorted Born approximation for subsurface reconstruction: truncation and uncertainties effects. *IEEE Transaction Geoscience and Remote Sensing*, 41, 66–74.
- [10] Persico, R., Bernini, R. and Soldovieri, F., 2005, The role of the measurement configuration in inverse scattering from buried objects under the Born approximation. *IEEE Trans. Antennas and Propagation*, 53, 1875-1887.
- [11] Bertero, M., 1989, *Linear inverse and ill-posed problems*. Adv. in Electron.and Electron. Phys. 45, pp. 1-120.
- [12] Pierri, R.; Liseno, A.; Solimene, R. and Soldovieri, F., 2006, Beyond physical optics SVD shape reconstruction of metallic cylinders. *IEEE Trans. Antennas and Propagation*, 54, 655-665.
- [13] F. Soldovieri, A. Brancaccio, G. Prisco, G. Leone, R. Pierri, 2008, A Kirchhoff based shape reconstruction algorithm for the multimonostatic configuration: the realistic case of buried pipes, *IEEE Transactions on Geoscience and Remote Sensing*, IGARSS Special Issue, 46, 3031 – 3038.
- [14] R. Solimene, F. Soldovieri, G. Prisco, R. Pierri, 2007, Three-Dimensional Microwave Tomography by a 2-D Slice-Based Reconstruction Algorithm”, *IEEE Geoscience and Remote Sensing Letters*, 4, 556 – 560.
- [15] E. Pettinelli, A. Di Matteo, E. Mattei, L. Crocco, F. Soldovieri, D.J. Redman, and A.P. Annan, 2009, GPR response from buried pipes: measurement on field site and tomographic reconstructions”, *IEEE Transactions on Geoscience and Remote Sensing*, 47, 2639 – 2645.
- [16] Chew, W. C., 1995, *Waves and Fields in Inhomogeneous Media*, Institute of Electrical and Electronics Engineers, Piscataway, NJ.
- [17] Soldovieri, F., Prisco, G., Persico, R., 2009, A strategy for the determination of the dielectric permittivity of a lossy soil exploiting GPR surface measurements and a cooperative target, *Journal of Applied Geophysics*, 67, 288-295.
- [18] Ahmad, F., Amin, M.G., Mandapati, G., 2007, Autofocusing of through-the-wall radar imagery under unknown wall characteristics. *IEEE Transactions on Image Processing*, 16, 1785–1795.
- [19] Martorella, M., Berizzi, F., Bruscoli, S., 2006, Use of genetic algorithms for contrast and entropy optimization in ISAR autofocusing. *EURASIP Journal on Applied Signal Processing*, 1–11.
- [20] Soldovieri, F., Prisco, G., Persico, R., 2008. Application of microwave tomography in hydrogeophysics: some examples, *Vadose Zone Journal*, 160–170.